FOSSEE, IIT Bombay
OpenFOAM Research Migration Project
August, 2023

# Response dynamics of a floating body subjected to waves

Akshay Suresh Shimpi[1] and Chandan Bose[2]

[1]MS Research Scholar, Department of Ocean Engineering, Indian Institute of Technology Madras
[2]Assistant Professor, Aerospace Engineering, School of Metallurgy and Materials, The University of Birmingham

September 3, 2023

## Synopsis

The numerical modelling of floating structures subjected to waves is gaining significant research attention in the field of naval, coastal, and ocean engineering. Wave-induced vibration of a floating body is investigated in this study using the Open-source CFD code - OpenFOAM. OlaFlow wave boundary condition is used to simulate the interaction of waves with a floating barge. The dynamic response of the freely floating barge is determined numerically and validated with the reference results from the existing literature. The present study reports a fluid-structure framework for predicting the response dynamics of a floating barge when subjected to wave-structure interactions.

## 1 Introduction

Floating structures are used for many purposes, such as substructures for oil and gas rigs, harbour piers, breakwaters, etc. Floating structures installed in shallow or deep water have the same problems caused by sea loads, corresponding mooring tensions, and station keeping. Floating structures such as Floating Production Storage and Offloading (FPSO), Semi-submersible, Spar, Tension Leg Platform (TLP), etc., are suited for deepwater. These structures are distinguished by several characteristics, such as functions, stability, motions, and load or volume capabilities. The dynamic response of the floating structure can be carried out numerically with simplified structure geometry and analytically derived wave loads. The potential flow solvers and nonlinear Computational Fluid Dynamics (CFD) solvers are employed to model fluid-structure interaction problems and simulate motion responses of floating structures in waves, wind, and current- thanks to significant advances in computing power and computational algorithm development. The early developed methods use frequency–domain analyses based on potential flow theories, which consider fluid as inviscid, and the nonlinear effect is not considered [1]. However, when the flow separation occurs around the body, and the nonlinear behaviour of floating bodies is the point of interest, inviscid and irrotational flow assumptions will not represent a realistic scenario for model testing. These methods are, therefore, limited to solving the motion of a floating body of a simple shape in small amplitude waves. It has been demonstrated that the interFoam coupled with body motion solver in OpenFOAM is capable of simulating wave-induced movements of floating objects [2–4]. Multiphase CFD numerical wave tank and wave generation and absorption techniques [5, 6] can reproduce open sea and experimental conditions.

The dynamic response of a freely floating barge with regular waves is validated in this study using OpenFOAM. A benchmark simulation is carried out with two different wave conditions for predicting the efficacy of the present fluid-structure interaction framework in accurately predicting the floating body response.

# 2 Governing Equations and Models

## 2.1 Problem definition

Ren et al. [7] validated the SPH model against experiments of nonlinear waves interacting with a freely floating barge. Here, the same test case is used to validate the OpenFOAM model. The experimental data included the time series of the motions (surge, heave and pitch) of a freely floating barge. Regular waves were tested during the physical test with a wave height of 4 cm and a wave period of 1.2 s.

## 2.2 Governing equations

The continuity equation and momentum equation are the fluid flow governing equations used, which are given below,

$$\nabla \cdot V = 0 \tag{1}$$

$$\rho(\frac{\partial V}{\partial t} + V \cdot \nabla V) = -\nabla p + \mu \nabla^2 V + \rho g \tag{2}$$

where V is the fluid velocity, $\rho$ is the fluid density, g is the acceleration due to gravity, P is the dynamic pressure, and $\mu$ is the dynamic viscosity of the fluid.

## 2.3 Volume of fluid (VOF) method

OpenFOAM uses the volume of fluid (VOF) method to capture the free surface of the interface between the two phases, air and water. In the VOF method, two phases have separate volume fractions $(\alpha)$. $\alpha$=1 dictates the cell is full of water; if $\alpha$=0, the cell is full of air and if 0<$\alpha$<1, the cell is a mixture of air and water. The density $\rho$ and viscosity $\mu$ in each cell is weighted by,

$$\rho = \alpha \rho_w + (1 - \alpha)\rho_a \tag{3}$$

$$\mu = \alpha \mu_w + (1 - \alpha)\mu_a \tag{4}$$

### 2.4 Geometry and Mesh

The two-dimensional case study of a freely floating barge was simulated in this study. The numerical setup for a freely floating barge is shown in figure 1. The barge is 30cm long, 20cm in height, and 42cm wide, with a mass of 12.6kg. The numerical setup consists of a 2-D numerical wave flume 4 m long with an initial water depth of 0.4 m. A piston-type wave generator is set on the left-hand side of the numerical wave flume, and a wave absorption boundary condition is placed on the other side to limit the presence of reflected waves in the flume. The deforming mesh method is used in this study as shown in figure 2. In the mesh morphing approach, mesh deforms while its topology remains the same. This method is used for small amplitude waves, as large amplitude results in deteriorated mesh quality.

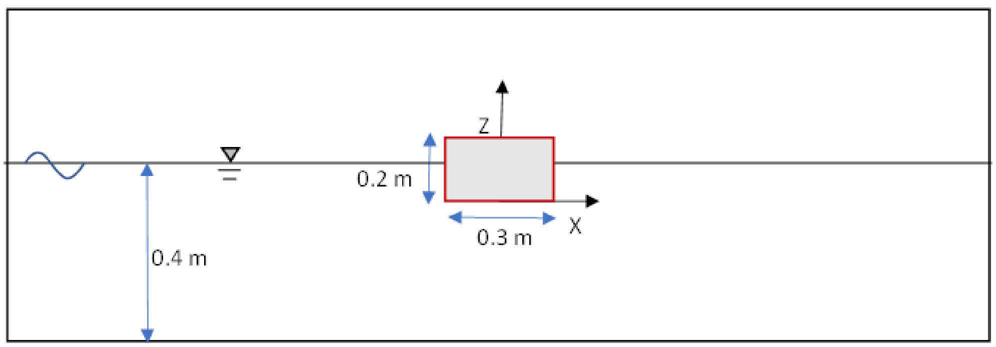


Figure 1: Numerical setup of a freely floating barge

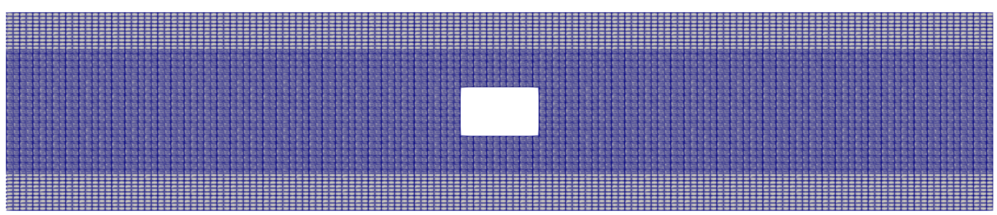

Figure 2: Deforming mesh

### 2.5 Solver setup

The olaDymFlow solver is an air-water two-phase flow solver used in this study. It solves the RANS equations using a finite volume discretization and the Volume of Fluid (VOF) surface capturing method. The simulation time step was adjusted at runtime with a maximum Courant number limit of 0.5. The second order CrankNicolson scheme was used for time marching. For each time step, three outer correctors were used along with two pressure correctors (no momentum predictor) per PISO loop. To avoid numerical instabilities, the floating body acceleration was relaxed by a factor of 0.8 and no acceleration damping was applied. This under-relaxation of body acceleration is a compromise between accuracy and stability. For deforming mesh simulations, cell deformations are allowed only within a region defined by an inner distance of 0.05 m and an outer distance of 0.35 m (relative to the moving body). A non-orthogonal corrector of 1 was used to account for the mesh non-orthogonality as a result of the mesh deformation. The numerical schemes used in this study are shown in Table 1.

Table 1: Numerical scheme

| Term | Scheme | Order |
|---|---|---|
| Gradient | Gauss linear | Second order |
| Divergence | Gauss vanLeer | Second order |
| Laplacian | Gauss linear corrected | Second order |
| Time | CrankNicolson | Second order |

### 2.6 Boundary conditions

Boundary conditions are set at the boundaries of the CFD domain in order to solve the governing equations. Table 2 lists the boundary conditions employed in the present study. The wave generation and absorption are made with an olaDymFlow solver with different values specified at the inlet and outlet of the computational domain. At the inlet, the volume fraction α and velocity are taken from first-order Stokes theory, and at the outlet, they are set to model the mean water level. The boundary conditions adopted in the study are given below.

Table 2: Bounday conditions

| Boundary | Pressure | Velocity | Volume fraction |
|---|---|---|---|
| Inlet | fixedFluxPressure | waveVelocity | waveAlpha |
| Outlet | fixedFluxPressure | waveAbsorption2DVelocity | zeroGradient |
| Bottom | fixedFluxPressure | NoSlip | zeroGradient |
| Atmosphere | totalPressure | pressureInletOutletVelocity | zeroGradient |
| Sidewalls | Empty | Empty | Empty |
| floatingObject | fixedFluxPressure | movingWallVelocity | zeroGradient |

## 3 Results and Discussions

The aim of this section is to predict the dynamic response of a freely floating barge. The experimental results of a regular wave interacting with a freely floating barge was validated with OpenFOAM results. The irregular wave simulation was also carried out to predict the responses in real sea conditions.

### 3.1 Grid convergence study

A grid-independence study was conducted to ensure the convergence of the solution as shown in figure 3. The background grid has been generated using the blockMesh utility in the OpenFOAM. The domain in the vertical direction has been divided into three regions, i.e. lower, central, and upper regions. The convergence is investigated using three different mesh configurations with the smallest cell sizes Δx= 0.133 m, 0.068 m, and 0.033 m. There is no significant change in the value of dynamic response for the three mesh sizes considered. Hence, a grid size of Δx=0.068 m and Δy= 0.011 m for the central region and 0.08 m for the lower and upper region was adopted for all the simulations considered in this study.

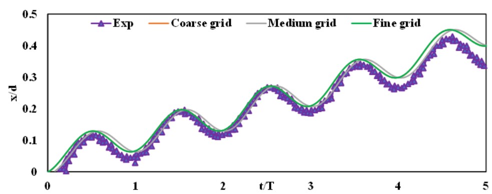


(a) Surge motion over time

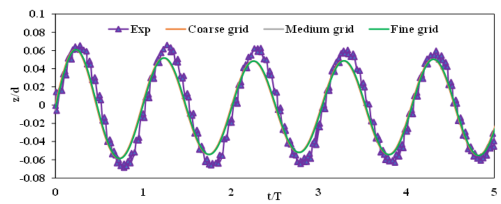


(b) Heave motion over time

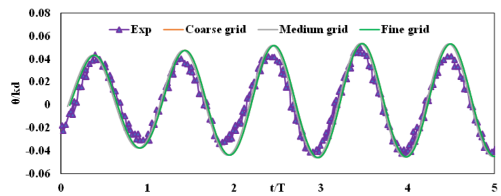


(c) Pitch motion over time

Figure 3: Spatial convergence of freely floating barge with regular waves

## 3.2 Temporal convergence study

To ensure numerical stability of the temporal terms,a temporal convergence study was conducted as shown in figure 4.

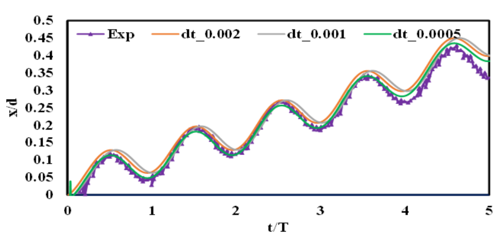


(a) Surge motion over time

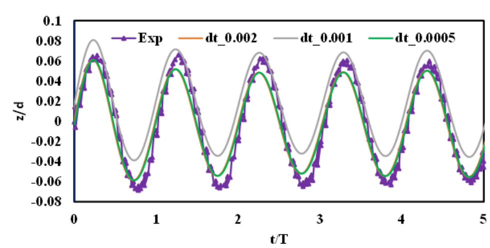


(b) Heave motion over time

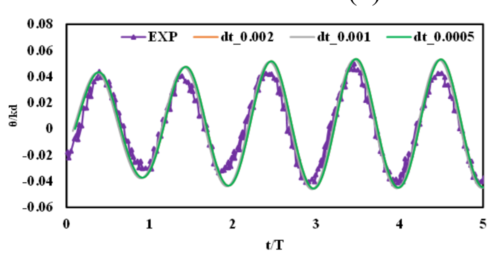


(c) Pitch motion over time

Figure 4: Temporal convergence of freely floating barge with regular waves

The adjustable time step was chosen in such a way that the maximum courant number was 0.5 for all the simulations. Three different time steps (Δt=0.002 s, 0.001 s, 0.0005 s) were considered. For better computational efficiency and less computational cost, a time step of 0.001 s was chosen for all the simulations performed.

## 3.3 Model validation study

Figure 5 shows the time histories of motion trajectories of freely floating barge results for the medium grid. Heave and pitch components show simple harmonic motion. Simple harmonic motion combined with drifting motion in the x direction can be seen for the surge motion. The drifting motion in the x-direction is due to mean drift forces. According to research by Mauro [8], the mean drift on a floating body is proportional to the square of the sum of the reflected and scattered wave height due to the moving body. Surge, heave, and pitch response calculated by OpenFOAM match the literature experimental results reasonably well. Figure 6 and Figure 7 show the different time instants of floating barge pressure and alpha water variation for regular waves. It can be seen that the barge firstly rotates clockwise and drifts rightwards with waves coming from the left. Then, following the rising surface on the right-hand side and falling on the left, it rotates anticlockwise and finally completes the whole cycle. Under inertia force, it continues to turn anticlockwise and drifts leftwards.

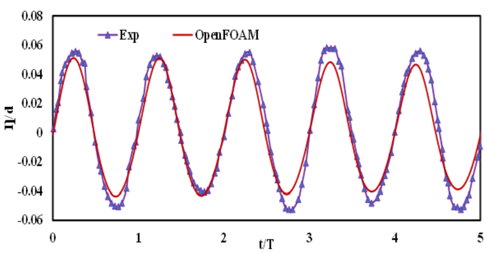


(a) Wave elevation over time

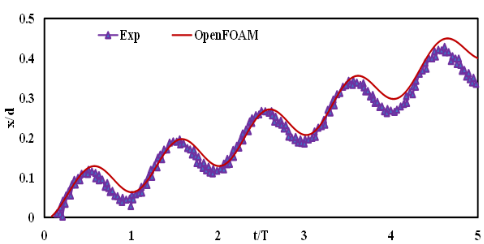


(b) Surge motion over time

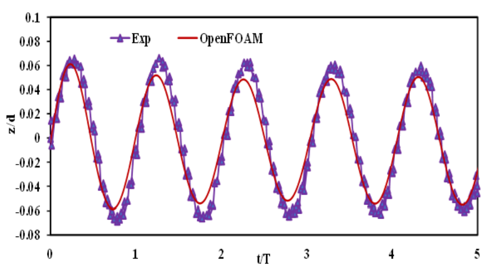


(c) Heave motion over time

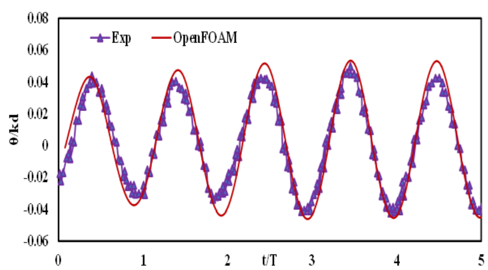


(d) Pitch motion over time

Figure 5: Time histories of motion trajectories of freely floating barge with regular waves

## 3.4 Freely floating barge with irregular wave

Waves in the natural ocean are seldom purely irregular. In order to simulate natural conditions, an irregular wave-generating theory is needed. First-order and second-order theories will suffice to represent the sea state to get more accurate results. A 2-D wave tank in which an irregular sea state

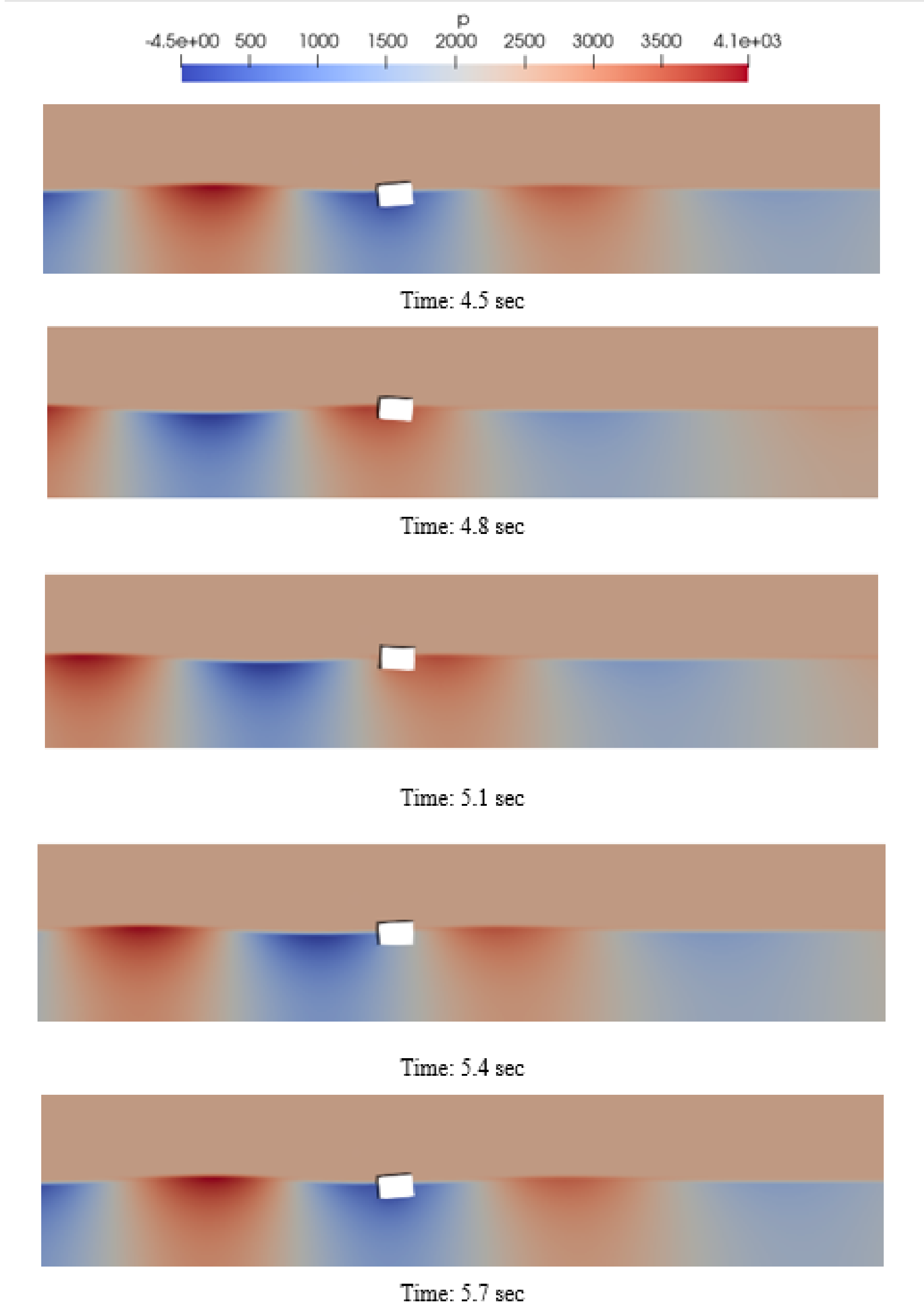


Figure 6: Different time instants of the interaction of regular waves with freely floating barge (pressure)

is generated with 842 wave components. No porosity is involved in the simulation performed in this study. Figure.8 shows time histories of motion trajectories of surge, heave, and pitch motion of freely floating barge with irregular waves.

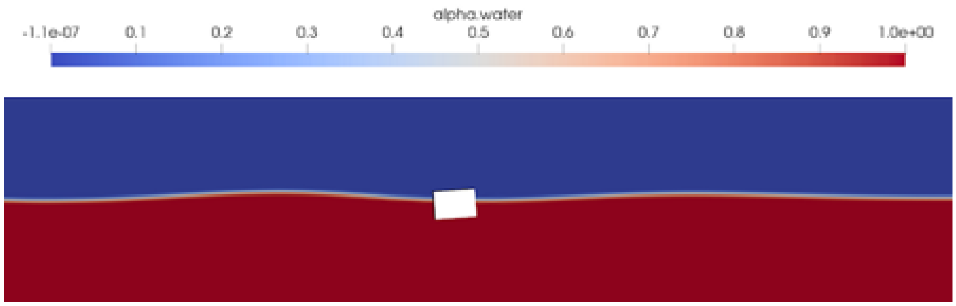


Time: 4.5 sec

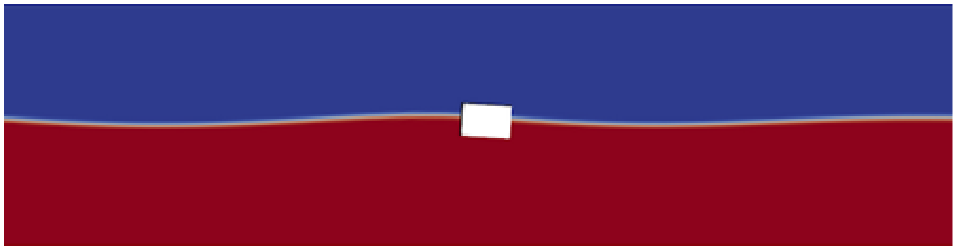

Time: 4.8 sec

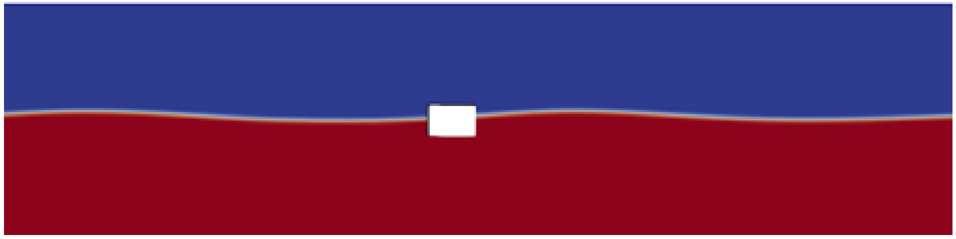

Time: 5.1 sec

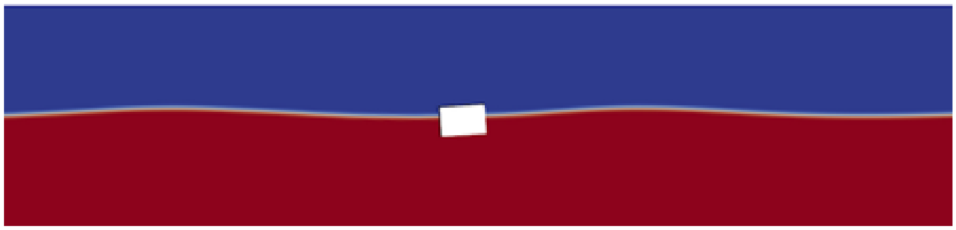

Time: 5.4 sec

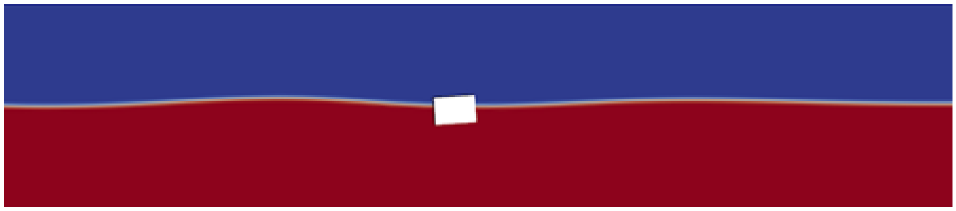

Time: 5.7 sec

Figure 7: Different time instants of the interaction of regular waves with freely floating barge (alpha water)

### 3.4.1 First order

First-order irregular waves are generated as a linear superposition of linear waves for a given number of components(N). This approach is physically correct, as most of the time, very small amplitudes are obtained by discretizing a real wave spectrum with a large number of components. Each of the components is defined by its wave height $H_i$, wave period $T_i$ , wave phase $\Psi_i$, and the direction of propagation ($\beta_i$). Free surface and orbital velocity components are given by,

$$\eta = \sum_{i=1}^{N} \frac{H_i}{2} cos(k_{xi}x + k_{yi}t - \omega_i t + \psi_i) \tag{5}$$

Irregular waves cause the floating body to experience complex and irregular motions. The body will move in various directions and orientations, pitching and heaving in response to the changing wave conditions. Figure 9 and figure 10 show the different time instants of the interaction of irregular waves with the freely floating barge. Irregular waves cause a significant impact on the body's center of gravity, body induces surging, and potentially lead to capsizing as the stability limits are exceeded.

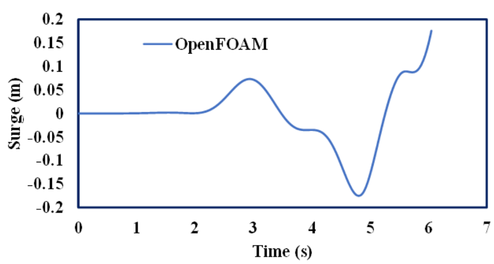


(a) Surge motion over time

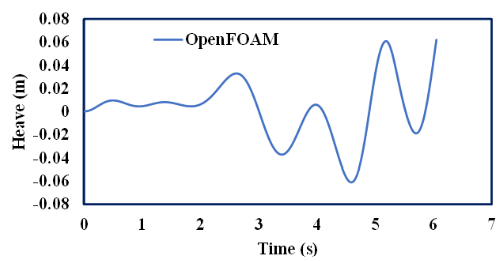


(b) Heave motion over time

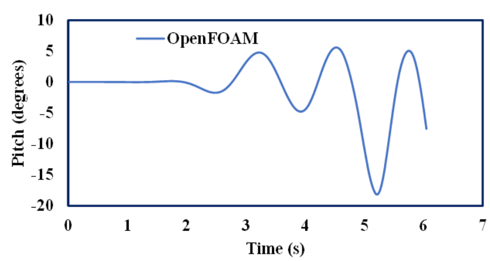


(c) Pitch motion over time

Figure 8: Time histories of motion trajectories of freely floating barge with irregular waves

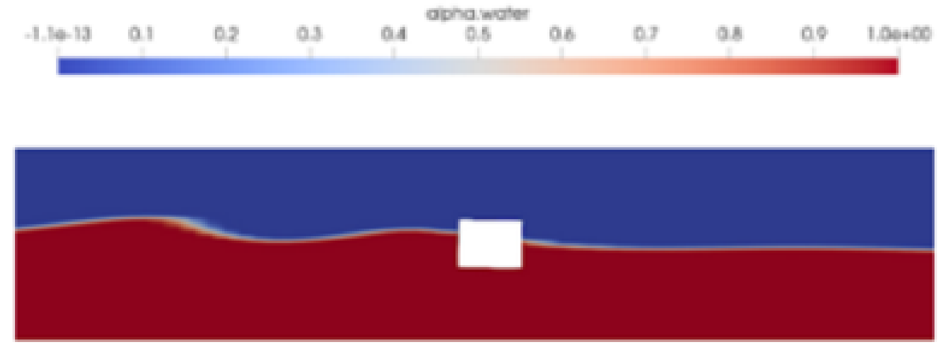


Time: 3.8 sec

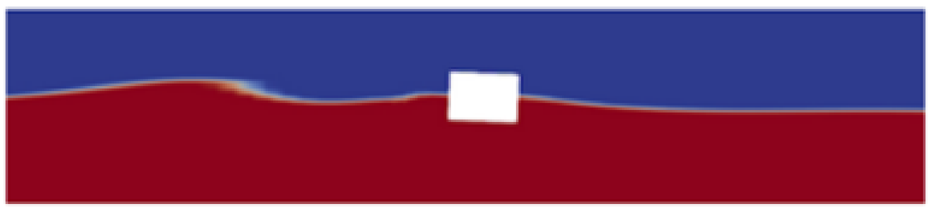

Time: 4.1 sec

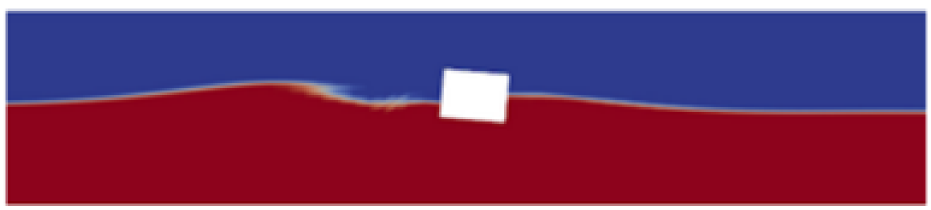

Time: 4.4 sec

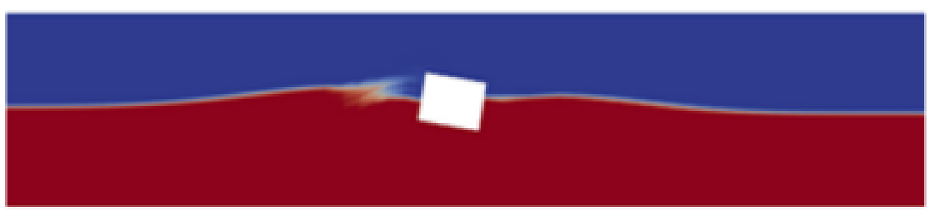

Time: 4.7 sec

Time: 5.0 sec

Figure 9: Different time instants of the interaction of irregular waves with freely floating barge (alpha water)

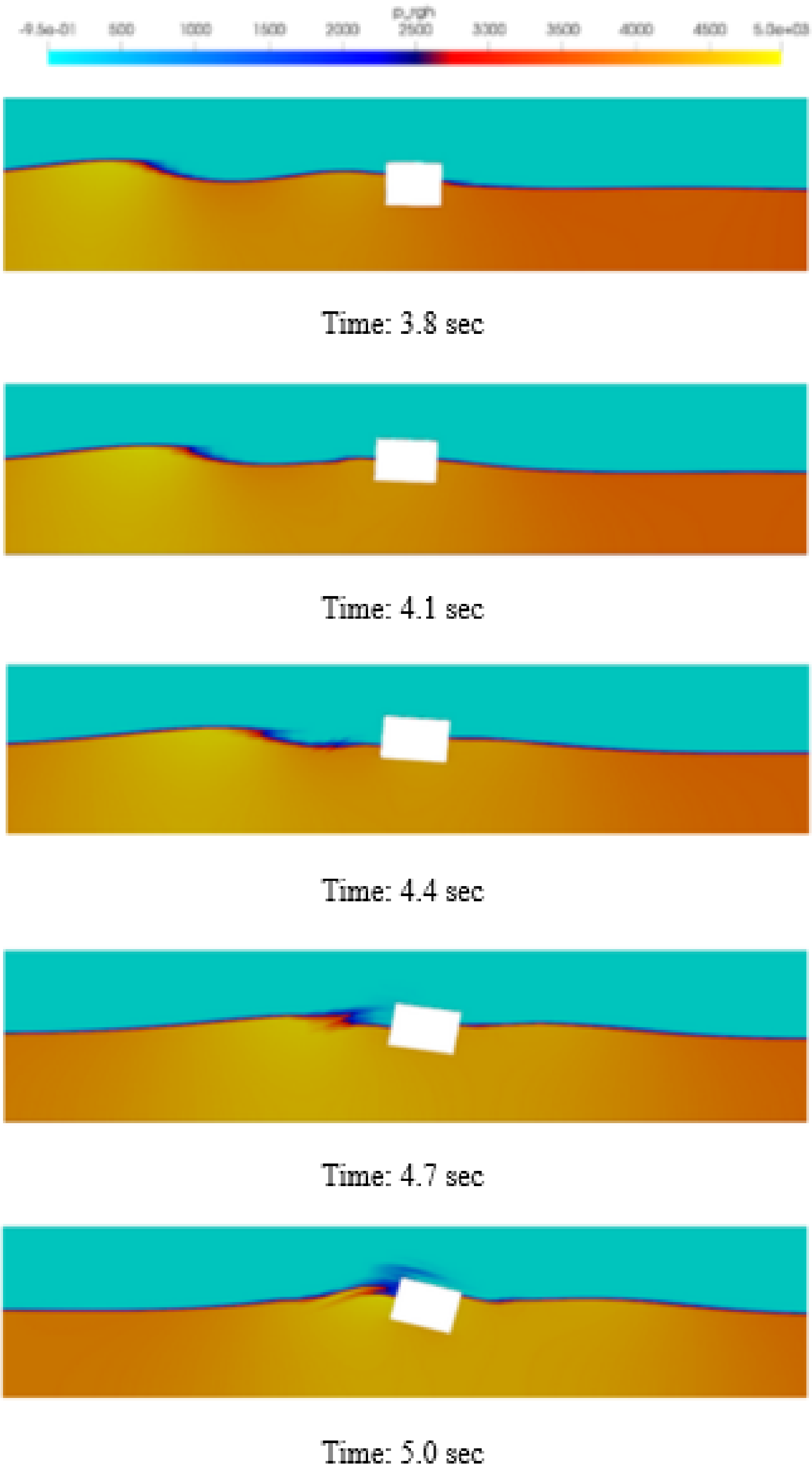


Figure 10: Different time instants of the interaction of irregular waves with a freely floating barge (pressure)

# 4 Conclusions

The present study investigates the dynamic response of a freely floating barge with regular and irregular waves using the finite volume open-source CFD code OpenFOAM. The response of freely floating barge matches reasonably well with the literature's experimental data. The model is found to be accurate in predicting the response of more complex structures like wave energy converters, oscillating water columns, etc.

# 5 Acknowledgement

I would like to express my gratitude to my mentor Dr. Chandan Bose for his guidance throughout my internship period. His deep knowledge of CFD and willingness to clear my doubts help me complete my internship within the stipulated time frame. He conducts weekly meetings throughout the internship period that help me a lot to put forth my suggestions and clear my doubts. I thank Prof. Manaswita Bose for the valuable suggestions rendered during the internship. I would like to express my gratitude to Mr. Krishna Kant and Mrs. Payel Mukharjee, Project manager of CFD-OpenFOAM Team FOSSEE for supporting me during the internship period. I would like to thank my fellow mate Mr. Rishab Sharma and Mr. Sochrate, research scholars IIT Madras to clarify my doubts. I would like to sincerely thank my family for their support during the work. Finally, I would like to thank the entire CFD-OpenFOAM FOSSEE Team for giving me this opportunity.

# References

[1] H. Sun, "A boundary element method applied to strongly nonlinear wave-body interaction problems," 2007.

[2] J. Palm, C. Eskilsson, G. M. Paredes, and L. Bergdahl, "Coupled mooring analysis for floating wave energy converters using cfd: Formulation and validation," *International Journal of Marine Energy*, vol. 16, pp. 83–99, 2016.

[3] N. Bruinsma, B. Paulsen, and N. Jacobsen, "Validation and application of a fully nonlinear numerical wave tank for simulating floating offshore wind turbines," *Ocean Engineering*, vol. 147, pp. 647–658, 2018.

[4] L. Chen, B. Basu, and S. R. Nielsen, "A coupled finite difference mooring dynamics model for floating offshore wind turbine analysis," *Ocean Engineering*, vol. 162, pp. 304–315, 2018.

[5] P. Higuera, J. L. Lara, and I. J. Losada, "Realistic wave generation and active wave absorption for navier–stokes models: Application to openfoam®," *Coastal Engineering*, vol. 71, pp. 102–118, 2013.

[6] N. G. Jacobsen, D. R. Fuhrman, and J. Fredsøe, "A wave generation toolbox for the open-source cfd library: Openfoam®," *International Journal for numerical methods in fluids*, vol. 70, no. 9, pp. 1073–1088, 2012.

[7] B. Ren, M. He, P. Dong, and H. Wen, "Nonlinear simulations of wave-induced motions of a freely floating body using wcsph method," *Applied Ocean Research*, vol. 50, pp. 1–12, 2015.

[8] H. Maruo, "The drift of a body floating on waves," *J. Ship Res.*, vol. 4, pp. 1–10, 1960.